High-vacuum versus "environmental" electron beam deposition

Albert Folch,[a] Jordi Servat, Joan Esteve, and Javier Tejada
Facultat de Física, Universitat de Barcelona, 08028 Barcelona, Spain

Miquel Seco
Facultat de Química, Universitat de Barcelona, 08028 Barcelona, Spain

Electron beam deposition (EBD) provides an inexpensive way to fabricate nanostructures of various materials in a scanning electron microscope (SEM). However, the purity of metals deposited from an organometallic precursor gas is impaired by simultaneously deposited carbon coming both from the organometallic molecule and the residual contamination gas in the SEM chamber. We discuss carbon-contamination EBD in a standard high-vacuum SEM and compare it to EBD of Au in an environmental SEM (ESEM). The ESEM allowed us to perform "environmental" EBD (E-EBD), i.e., EBD in the presence of an environmental gas (1–10 Torr) in addition to the organometallic precursor gas. We built a simple device that contains a reservoir for the organometallic precursor and goes on the sample stage of the ESEM. With this device we were able to highlight the advantages of E-EBD over conventional, high-vacuum EBD. We discuss the basic chemical reactions underlying the E-EBD process. © *1996 American Vacuum Society.*

I. INTRODUCTION

Conventional deposition techniques currently used in the fabrication of micron or submicron structures (e.g., microelectronics devices) do not allow the deposition of materials on a very small area of the substrate. Instead, materials are deposited over the whole substrate and the pattern is defined afterwards by removing material from the adjacent areas. The creation of a given pattern involves several tedious steps (such as masks, resists, photo- or electron-beam lithography, lift-off, and/or selective etching) which result in costly processes and generally require planar substrates. The cost is usually justified by the large number of devices produced in parallel. However, alternative techniques are sought for many applications where a few devices suffice. Also, it is particularly important for microsensor engineering to develop patterning techniques that are compatible with nonplanar substrates.

Electron beam deposition (EBD) is an inexpensive technique suitable for the fabrication of structures of different sizes, shapes, and materials in the submicron or nanometer scale. In the presence of a surrounding gas, a finely focused electron (e^-) beam is observed to cause the deposition of material from the gas only in the area irradiated by the beam. In EBD, materials are patterned and deposited *simultaneously*. This one-step process is comparatively inexpensive. Since it is maskless and resistless, it has the advantage that it allows patterning on nonplanar substrates. On the other hand, since it is induced locally, it is time-consuming. Another disadvantage concerns the purity of the deposits, as will be discussed later.

The observation of EBD is not new. The formation of carbonaceous films on surfaces upon electron bombardment in vacuum haunted researchers for more than 30 years.[1] Ennos[2] identified specimen contamination in the electron mixcroscope produced by the interaction between the bombarding e^- and the organic molecules adsorbed on the specimen surface. Broers *et al.*[3] were the first to deposit nanometerscale carbon-contamination structures in a scanning transmission electron microscope (STEM). We describe our studies on carbon-contamination EBD in Sec. II. By allowing a small pressure of an organometallic vapor in the chamber of a scanning electron microscope (SEM), Matsui and Mori[4] deposited 0.15-μm-wide metallic lines. The principle of EBD is sketched in Fig. 1. The dissociation of some or all of the gas molecules that happen to adsorb on the irradiated spot results in the formation of a deposit consisting of the nonvolatile remains from that dissociation.[5-8] The deposition rate depends on the total e^--beam current density at the beam spot, on the effective adsorption rate of the precursor gas molecules onto the substrate, and on the probability for an electron to cause EBD of a molecule. In addition, the beam current density depends not only on the beam spot size but also on the rate of emission of secondary and backscattered electrons, which also contribute to the process. Recently, EBD has been demonstrated with a scanning tunneling microscope (STM) operated in field-emission mode.[9] For our work we used SEMs because of their flexibility and availability. We developed an instrumentally simple device to perform EBD without needing to modify the SEM chamber for introduction of the precursor gas. We call this device the "EBD cell" (Sec. III). We used it to demonstrate "environmental" EBD (E-EBD). This approach has several advantages over conventional EBD (Sec. IV). The growth process is analyzed in Sec. V.

[a]Author to whom all correspondence should be addressed. Present address: Microsystems Technology Laboratory, Massachusetts Institute of Technology, Cambridge, Massachusetts; Electronic mail: afolch@mit.edu
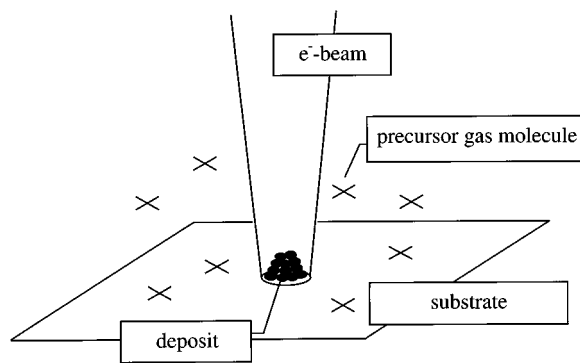
FIG. 1. Principle of EBD. A focused e^- beam induces a chemical change on the precursor gas molecules that are adsorbed on the irradiated spot.

II. CARBON-CONTAMINATION EBD

One may straightforwardly carry out an EBD experiment by means of a standard SEM operated at low beam currents ($\sim$10–50 pA) and high beam energies ($\sim$15–30 keV). These parameters are generally not critical. A flat sample with a thin film of sputtered gold to avoid charging will generally suffice. A rough sample will make the observation of the submicron-sized deposits difficult. A requirement is that the e^--beam be well focused. Stopping the e^- beam on a given spot for a few minutes will typically cause the growth of a submicron-diameter column or tip. The growth rate varies greatly from one SEM to another, probably due to different residual gas pressures and/or composition. If the growth rate is very slow, beam instabilities and/or drifts will prevent the formation of a fine column.

We deposited columns and lines on a thin film of Au ($\sim$1000 Å) on Si with an SEM operating at a base pressure of 5×10^{-5} Torr. A microfabricated trench in the Si substrate served as a landmark for easy location of the deposits. A set of tips is shown in Fig. 2(a). A nearby dust speck helped to finely focus the e^- beam. The tips were grown for periods of time varying from 30 s to 10 min, and with beam currents and acceleration voltages ranging 10–30 pA and 15–40 kV, respectively. The apparent conical shape can be attributed to instabilities of the e^- beam that effectively spread the e^- beam spot, such as noise in the deflection electrodes, mechanical vibrations, and thermal drifts. The capability to write lines is demonstrated in Fig. 2(b).

An interesting observation is that these contaminants can be present even at lower pressures, as in a scanning Auger microanalysis (SAM) system operating at a base pressure of 10^{-9}–10^{-10} Torr. On an indium-tin-oxide (ITO) sample previously cleaned by Ar^+ sputtering (0.5 min, 20 μA/cm^2, 2 keV) we exposed a 75 μm $\times$ 50 μm area by raster scanning the e^- beam of the SAM for 16 hours. After this period of time, the exposed area appeared blackened in an electron micrograph and its Auger analysis revealed the presence of carbon only. The black appearance can be explained by the particularly low secondary electron emission rate of carbon. The thickness of the deposit has to be at least several nanometers in order to screen the Auger emission of the indium, tin,
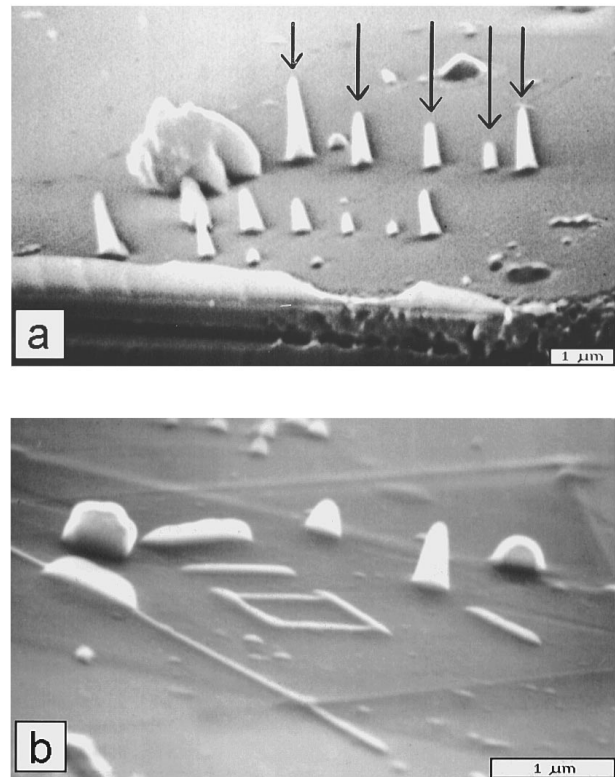

FIG. 2. Illustrative examples of carbon-contamination EBD. The white scale bar represents 1 μm. To deposit a tip, the beam is focused on the desired spot for a certain amount of time. (a) A set of tips is grown near a dust speck. The series of 5 tips in a row indicated by arrows was grown for periods of time of (from left to right) 10, 5, 2.5, 1, and 5 min. Beam current and energy were 30 pA and 40 keV, respectively. (b) The four 1-μm-long lines forming the square were deposited in 4 min each with a single line scan (4 min/μm) at 8 pA and 15 keV. The two broader, taller lines were deposited under the same beam conditions but 6 times slower (24 min/μm).

and oxygen in the underlying ITO substrate. Therefore, the amount of carbon present on any given sample is overestimated because the analyzing e^- beam simultaneously causes deposition of carbon. This problem poses a challenge to the characterization of very small deposits. Furthermore, the composition of a spot or column deposited with a stationary e^- beam cannot be analyzed with an e^- beam of similar resolution, since the analysis is comparatively slow and is severely affected by drifts. Usually, since the efficiency of Auger electron excitation is very low, high beam currents ($\sim$1 nA) are used in Auger analysis as compared to EBD ($\sim$10 pA), which results in bigger beam spot sizes. A partial solution to this problem is to analyze large deposits made by rastering the e^- beam across a large area ($\sim$100 μm^2).

III. ORGANOMETALLIC EBD: THE "EBD CELL"

The nature of the precursor gas determines the composition of the deposits. Metals, for instance, can be deposited from organometallic precursor gases.[4–8] Unfortunately, the purity of the deposits is affected by undesired deposition of carbon coming not only from the residual contamination
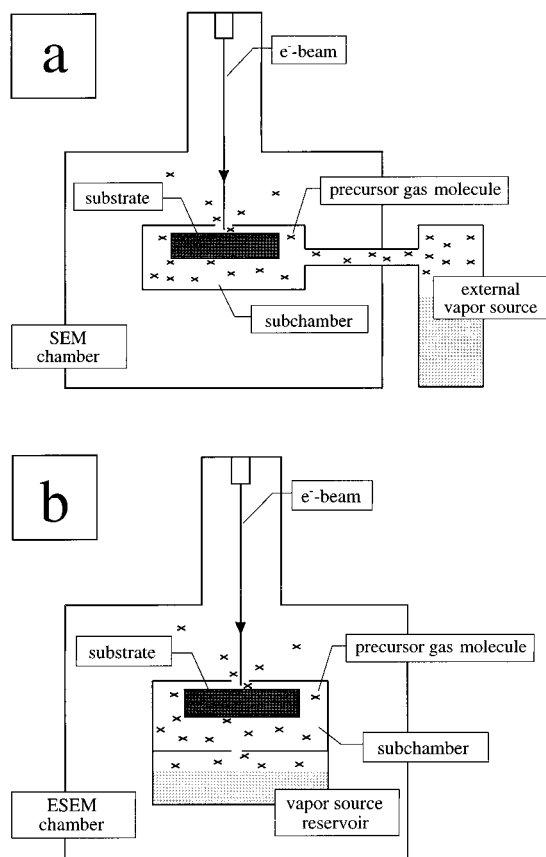
FIG. 3. Schematic of (a) the usual subchamber setup for EBD, and (b) our "EBD cell" setup. The environmental gas, not depicted for clarity, fills up the whole ESEM chamber.

gases, as discussed in Sec. II, but also from the organometallic precursor compound. Unfortunately also, since high vacuum is required for operation of the SEM, the precursor gas must be allowed inside the SEM chamber in small quantities. This results in low growth rates. Generally, the gas is introduced from an external source into a subchamber (containing the sample) within the SEM chamber [see Fig. 3(a)].[4-6] Some authors used a gas nozzle directed onto the sample.[7] The SEM chamber must be modified to accommodate a gas feedthrough, which may represent a serious inconvenience.

It is important to realize that high precursor gas pressures are desirable not only to obtain high growth rates but also to minimize carbon-contamination incorporation. At very low precursor gas pressures carbon deposition dominates and results in grossly impure deposits. Therefore, there is an essential incompatibility between the high vacuum requirements of conventional SEMs and the desired purity of the deposits.

To avoid hardware modifications to the SEM, we made a small device that acts as an *internal* vapor source and goes on the SEM sample stage. We call this device an "EBD cell" [see Fig. 3(b)]. The EBD cell is a 3.5-cm-diameter two-chamber assembly: one subchamber for the sample and a reservoir for the precursor material. Three screws hold the two chambers together and a sealing Viton O-ring in be-

tween. The vapors of the precursor material leave the reservoir through a fixed small aperture (which we call the "reservoir aperture"), enter the sample subchamber and escape through another fixed aperture (the "sample aperture") that exposes the sample to the e^- beam. Thus some gas molecules adsorb on the sample spot that is being irradiated by the beam. The apertures were TEM diaphragms (with hole diameters ranging from 5 to 500 μm) glued with silver paint on 1-mm-diameter holes machined on top of each chamber. In practice, the choice of aperture sizes is limited by (a) the desired growth rate, (b) the sample area accessible by the beam, (c) the amount of precursor material given its vaporization rate, and (d) the vacuum requirements of the SEM. Since the apertures are removable, this is straightforwardly determined by trial and error. Variable apertures, pressure gauges and an electrode gauge could be implemented for a precise control and *in situ* variation of the growth rates.

To eliminate the vacuum constraints we used an environmental SEM (ESEM).[6] With the ESEM it is possible to image in the presence of up to 20 Torr of certain gases. The detection of secondary electrons for imaging is possible due to the highly ionized state of the environmental gas above the beam spot. We used Ar, H_2O 2O, and a mixture of 80% Ar and 20% O_2 (Ar/O_2) as environmental gases.

The performance of the cell was first optimized by experimenting with EBD of Fe from iron pentacarbonyl, $Fe(CO)_5$, a liquid with a vapor pressure of 3 Torr at 20 °C.[11] Then we deposited Au at room temperature from $Au(CH_3)_2$(hexafluoroacetylacetonate), a liquid with a vapor pressure of 700 mTorr at 20 °C (hereafter referred to as DMGHFAC). We emphasize that both the organometallic precursor, emanating from the reservoir, and the environmental gas (Ar,H_2O, or Ar/O_2), filling up the whole ESEM chamber, were present during deposition.

In all the experiments reported here, the EBD cell was used in combination with the ESEM, but it has been used successfully in high vacuum in a standard SEM as well.[11] A few droplets of DMGHFAC last ~30 min in the reservoir at environmental pressures of ~1–3 Torr if the reservoir aperture and the sample aperture are 50 μm and 1 mm in diameter, respectively. This yields growth rates of around 40 nm/s.[8] A key feature of the EBD cell performance is that at our environmental gas pressures (~1 Torr) the precursor gas molecules leave the subchamber by diffusion, rather than ballistically as in previous subchamber setups in vacuum. This yields low evaporation rates of the precursor compound while allowing a large sample area exposed to the e^- beam.

IV. ENVIRONMENTAL EBD OF HIGH-ASPECT-RATIO NANOSTRUCTURES

The concept of environmental EBD (E-EBD), i.e., EBD in the presence of an environmental gas in addition to the precursor gas, can be advantageous for several applications. This process was recently applied to reduce carbon incorporation in EBD of Au.[8] The environmental gas was either Ar, H_2O, or Ar/O_2. The presence of Ar/O_2 or H_2O reduced the C content of the deposits (as measured with Auger electron
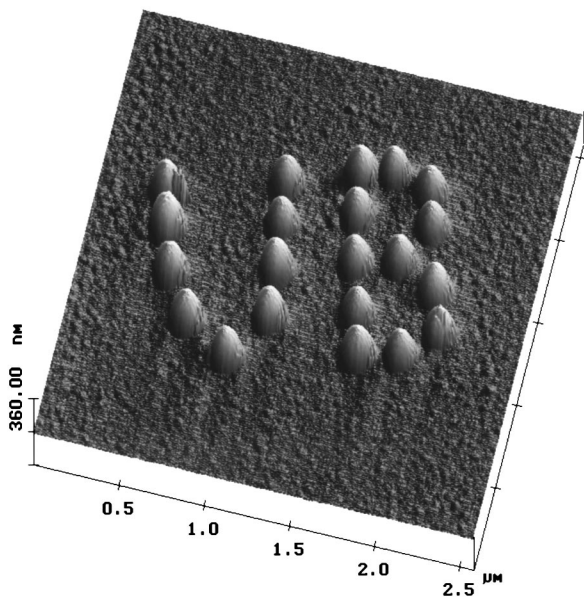
FIG. 4. AFM image of EBD columns deposited on Si from DMGHFAC vapor at 30 keV. The columns appear convoluted with the AFM tip, as manifested by identical sidewall features on each column.

FIG. 5. EBD columns deposited on top of pyramidal AFM tips. The white scale bar represents (a) 5 μm and (b) 1 μm.

spectroscopy) whereas Ar did not. Moreover, the Au content increased with increasing H_2O or Ar/O_2 pressure, whereas it was significantly affected by changes in Ar pressure. The highest Au contents (50%) were achieved under 10 Torr of Ar/O_2. With H_2O vapor, the overall contents were smaller (up to 20% under 3 Torr). Very low Au contents (~ 2–3 %) were systematically observed in the absence of environmental gas. This indicated a large amount of hydrocarbon residual gases in the ESEM chamber and highlighted the accomplishment of 50% Au composition by means of E-EBD.

The concept of E-EBD can also be applied to create high-aspect-ratio nanostructures. Since the ESEM is able to operate at high environmental gas pressures (0–20 Torr), it is inherently compatible with higher precursor gas pressures than standard high-vacuum SEMs. This can yield very high growth rates and aspect ratios. We achieved linewidths of ~ 100 nm despite the high gas pressures. An example is shown in Fig. 4. A pattern of columns reading "UB" was deposited in 5 s/column from DMGHFAC on Si under 2 Torr of Ar/O_2 and with a 30 keV beam. The columns have an average height of 180 nm, which yields a growth rate of 36 nm/s. The widths (~ 100 nm) were measured with an SEM since in the atomic force microscope (AFM) image the columns appear wider than they really are due to convolution with the AFM tip. Since every column has the same rough features on its right sidewall, one can conclude that it is a feature present on the AFM tip itself. This suggests that arrays of EBD columns could be used as calibration tests to know the exact shape of an AFM tip.

The same procedures needed to create column structures such as those in Fig. 4 are applicable when the substrate is not flat. We were able to deposit >4-μm-high, 0.1-μm-thick columns from DMGHFAC on top of commercial microfab-
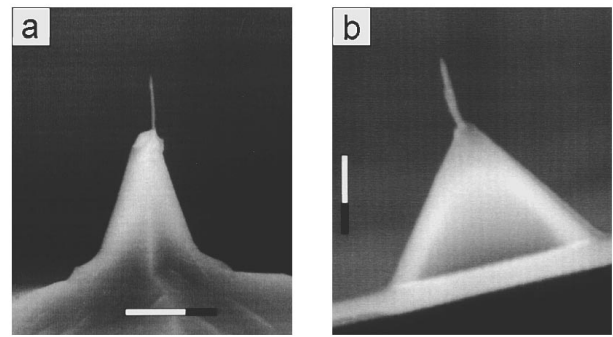
ricated AFM tips. Indeed, the unique capability of EBD for patterning nonplanar substrates caught the attention of STM and AFM researchers very early because sharp, high-aspect-ratio tips are critical in several applications.[12] Two examples are shown in Fig. 5. The deposition parameters were the same as in Fig. 4. The tips are not perfectly straight because the deposition of each tip was done with several short exposures (~ 5 s) to allow re-focusing of the beam between exposures. This was done to avoid broadening of the column. Tip heights are (a) 4 μm and (b) 1.5 μm.

Last but not least, with E-EBD it is possible to fabricate nanostructures on bulk insulators, such as the silicon nitride pyramid in Fig. 5(b), because in the ESEM the sample is continuously discharged through the ionized environmental gas.

V. DISCUSSION

It is important to note that the ESEM itself is not essential to the concept of EEBD. Similarly, we believe that the addition of a reactive gas to reduce carbon incorporation during EBD may as well be implemented in high vacuum. One could, for example, direct two nozzles to a sample in a high-vacuum SEM, one transporting the organometallic compound and another one transporting pure O_2. The composition of the deposits is probably determined by the ratio of the flows or partial pressures of the two gases. Furthermore, we expected electron scattering at our high environmental gas pressures to broaden the EBD features. However, we observed no dependence between environmental gas pressures <5 Torr and the width of the EBD features, which was routinely 100 nm or less (see Figs. 4 and 5). This is in accordance with the ESEM's surprisingly high resolution. Danilatos[13] has suggested that the beam is self-focused by a concentric plasma sheath, and its associated electrostatic field, around the beam. As noted above, in any case, lower pressures of similar mixtures of gases could be used in a high-vacuum EBD setup to deposit features at a slower rate and higher resolution. We stress that the concept of E-EBD is applicable to STM-EBD as well.

The composition of the deposits is virtually independent of the e^- beam energy for the values typically used in SEM imaging (~ 10–40 keV). This observation rules out the pos-

sibility that substrate heating by the impinging electrons plays a significant role in the EBD mechanism, as the heating effect increases with increasing energy. Essentially, EBD of a gaseous molecule is the rupture of one or more of the chemical bonds within the molecule by one or more high-energy electrons (> 1 keV), resulting in a solid deposit. Typical bonds in an organic molecule such as C-C, C-H, or C-O have energies of 3.25, 3.43, and 4.31 eV, respectively. Hence a high-energy electron cannot be used to selectively rupture the chemical bonds present in an organic molecule. The dynamic role of the continuously changing surface has not been investigated yet to our knowledge.

We explain our results on E-EBD by noting that highly reactive species are generated by the dissociation of the precursor gas molecules adsorbed on the substrate as well as by the ionization of environmental gas molecules above the surface. Thus, simultaneously with deposition, C in the deposits can be desorbed as CO or CO_2 molecules if an environmental gas supplies the oxygen ions or molecules necessary for that reaction to occur. Ar/O_2 is more effective than H_2O at doing so due to its richer presence of O at the compared pressures. That is, a total pressure of 10 Torr of Ar/O_2 (80%/20%) represents a partial pressure of 2 Torr of pure O_2. Thus the density of O atoms in 10 Torr of Ar/O_2 is twice as high as that in 2 Torr of H_2O, and accordingly it yields superior Au contents. Pure O_2, which could not be used for safety reasons,[14] should yield higher Au contents at similar environmental gas pressures. Finally, in our opinion the inert nature of Ar satisfactorily explains that Ar does not create a reactive environment.

A key observation is that in our experiments on organometallic EBD with DMGHFAC there is no trace of F or O in the Auger analysis of the deposits for standard e^- beam current and acceleration voltage deposition parameters (see Ref. 8). Since high-energy electrons break all bonds unpreferentially, the above observation suggests that the organometallic molecule is fully dissociated into its atomic constituents by the e^- beam. Rather than two or more inert molecules, the outcome of the dissociation is a set of highly reactive ions, probably monatomic, the recombination of which produces the observable deposit along with volatile compounds. The creation of F_2 and O_2 molecules, for example, satisfactorily explains the absence of F and O in the Auger analysis of the deposits. In general, any reducing species present in the environmental plasma (such as H^+ from H_2O) will also contribute to their desorption. In the case of Ar, it is probably a small partial pressure of other residual gases (such as H_2O) that provides the necessary reducing agents. The Au:C:O:F:H atomic ratios in the DMGHFAC molecule are 1:7:2:6:8. Although H cannot be detected with Auger spectroscopy, the above arguments should also hold true for H. For this reason, we expect the deposit to be composed of only Au and C in a Au:C ratio of 1:7 (12.5% Au) *at least*. Therefore, in EBD of Au with DMGHFAC, Au contents smaller than 12.5% must be attributed to simultaneous carbon-contamination deposition from residual hydrocarbon gases in the SEM chamber.

Probably, in high vacuum the organometallic compound does not fully dissociate under certain low-electron-density conditions. Indeed, assuming full dissociation the most likely recombination favors the creation of two desorbing CO molecules, other recombinations being far less likely. Accordingly, it should contain up to 16.7% Au (Au:C=1:5) *at most*. However, higher Au contents have been reported by others.[5,6] This suggests that in high vacuum the molecule is not fully dissociated and that bigger species are desorbed. We could not investigate ranges of pressure <0.1 Torr with the ESEM because of its inaccuracy in pressure control. We explain the higher degree of dissociation observed in E-EBD as compared to conventional high-vacuum EBD by noting that in E-EBD the precursor gas molecules adsorbed on the e^- beam spot are bombarded by electrons as well as by reactive ions.

VI. CONCLUSIONS

We have described an innovative setup for EBD that requires no modifications to the SEM chamber. It consists of a small subchamber with a built-in reservoir for the precursor compound, thus eliminating the need for a feedthrough for introduction of the precursor gas from outside the SEM chamber. With this device we had previously introduced the concept of environmental EBD (E-EBD). The composition of Au deposits can be substantially improved by a judicious choice of the environmental gas and the growth rates can be much higher than in high-vacuum EBD, which yields high-aspect-ratio nanostructures. Here we discussed its advantages and analyzed the beam-induced reaction mechanisms of E-EBD as compared to high-vacuum EBD.

[1]R. L. Stewart, Phys. Rev. **45**, 488 (1934); J. H. L. Watson, J. Appl. Phys. **18**, 153 (1947); J. Hillier, J. Appl. Phys. **19**, 227 (1948); K. M. Poole, Proc. Phys. Soc. London B **66**, 542 (1953).
[2]A. E. Ennos, Brit. J. Appl. Phys. **4**, 101 (1953); **5**, 27 (1954).
[3]A. N. Broers, W. W. Molzen, J. J. Cuomo, and N. D. Wittels, Appl. Phys. Lett. **29**, 596 (1976).
[4]S. Matsui and K. Mori, Jpn. J. Appl. Phys. **23**, L706 (1984).
[5]H. W. P. Koops, R. Weiel, D. P. Kern, and T. H. Baum, J. Vac. Sci. Technol. B **6**, 477 (1988).
[6]K. L. Lee and M. Hatzakis, J. Vac. Sci. Technol. B **7**, 1941 (1989).
[7]K. T. Kohlman-von Platten, J. Chlebek, M. Weiss, K. Reimer, H. Oertel, and W. H. Brünger, J. Vac. Sci. Technol. B **11**, 2219 (1993).

[8]A. Folch, J. Tejada, C. H. Peters, and M. S. Wrighton, Appl. Phys. Lett. **66**, 2080 (1995).

[9]R. M. Silver, E. E. Ehrichs, and A. L. de Lozanne, Appl. Phys. Lett. **51**, 247 (1987); M. A. McCord, D. P. Kern, and T. H. P. Chang, J. Vac. Sci. Technol. B **6**, 1877 (1988).

[10]G. D. Danilatos, Micron Microsc. Acta **14**, 307 (1983).

[11]A. Folch, Ph.D. thesis, Universitat de Barcelona, Spain, 1994.

[12]Y. Akama, E. Nishimura, A. Sakai, and H. Murakami, J. Vac. Sci. Technol. A **8**, 429 (1990); D. Keller, D. Deputy, A. Alduino, and K. Luo, Ultramicroscopy **42−44**, 1481 (1992).

[13]G. D. Danilatos, Adv. Electron. Electron. Phys. **71**, 109 (1988).

[14]The hydrocarbon oil of our ESEMs mechanical pump could ignite in contact with pure O_2. A perfluorinated polyether oil should be used instead to pump pure O_2.